Journal of Medicinal Chemistry

Brief Article

Highly potent and isoform-selective dual-site-binding tankyrase/Wnt signaling inhibitors that increase cellular glucose uptake and have anti-proliferative activity

AMIT NATHUBHAI, Teemu Haikarainen, Jarkko Koivunen, Sudarshan Murthy, Françoise Koumanov, Matthew D. Lloyd, Geoffrey D. Holman, Taina Pihlajaniemi, David Tosh, Lari Lehtiö, and Michael D. Threadgill

J. Med. Chem., **Just Accepted Manuscript** • DOI: 10.1021/acs.jmedchem.6b01574 • Publication Date (Web): 16 Dec 2016

ACS Publications

Journal of Medicinal Chemistry is published by the American Chemical Society. 1155 Sixteenth Street N.W., Washington, DC 20036

Highly potent and isoform-selective dual-site-binding tankyrase/Wnt signaling inhibitors that increase cellular glucose uptake and have anti-proliferative activity.

Amit Nathubhai,[*†] Teemu Haikarainen,[‡] Jarkko Koivunen,[‡] Sudarshan Murthy,[‡] Françoise Koumanov,[§] Matthew D. Lloyd,[†] Geoffrey D. Holman,[§] Taina Pihlajaniemi,[‡] David Tosh,[§] Lari Lehtiö,[‡] Michael D. Threadgill[†]

[†] Drug and Target Discovery, Department of Pharmacy and Pharmacology, University of Bath, Bath BA2 7AY, U. K.,
[‡]Faculty of Biochemistry and Molecular Medicine, Biocenter Oulu, University of Oulu, PO Box 5400, 90014 Oulu, Finland
[§]Department of Biology and Biochemistry, University of Bath, Bath BA2 7AY, U. K.

KEYWORDS: Tankyrase, PARP, Glucose uptake, Wnt signaling, Crystal structure, Insulin.

ABSTRACT: Compounds **13** and **14** were evaluated against eleven PARP isoforms to reveal that both **13** and **14** were more potent and isoform-selective towards inhibiting tankyrases (TNKSs) than the "standard" inhibitor **1** (XAV939)[5], *i.e.* IC_{50} = 100 pM *vs.* TNKS2 and IC_{50} = 6.5 μM *vs.* PARP1 for **14**. In cellular assays, **13** and **14** inhibited Wnt-signaling, enhanced insulin-stimulated glucose uptake and inhibited the proliferation of DLD-1 colorectal adenocarcinoma cells to a greater extent than **1**.

INTRODUCTION

Tankyrases (TNKSs) are members of the poly(ADP-ribose)-polymerase (PARP) family of seventeen enzymes that use NAD^+ as a substrate to transfer ADP-ribose units to target proteins.[1] There are two human isoforms, TNKS1 and TNKS2. Target proteins include telomere repeating binding factor-1 (TRF1),[2,3] nuclear mitotic apparatus protein (NuMA)[4] (essential for the resolution of chromatids during mitosis) and axin, the limiting component of Wnt / β-catenin signaling.[5] Increased Wnt signaling correlates with the overexpression of TNKSs in several human cancers.[6-9] Inhibition of TNKSs is reported to lead to stabilization of axin and decreased nuclear β-catenin-driven proliferation of cancer cells.[10] Epidemiological studies show that patients with Type-2 diabetes are at higher risk of developing site-specific cancers[11] but the precise mechanisms that link diabetes to cancer remain unclear. The axin-TNKS-KIF3A complex is required for insulin-stimulated translocation of GLUT4 to the cell memembrane.[12] Insulin-regulated aminopeptidase (IRAP) is also a binding partner and target protein of TNKSs.[13] Together, IRAP and TNKSs can enhance insulin-stimulated exocytosis of GLUT4, which could result in increased uptake of glucose.[13] TNKS-knockout mice display increased sensitivity to insulin and reduced adiposity and pan-PARP inhibitors have been used to investigate the role of TNKSs in studies on the translocation of GLUT4.[14] Inhibitor **1** (XAV939)[5] (Fig. 1) has been extensively used as a tool to inhibit TNKSs and of Wnt / β-catenin signaling[5] but lacks the required isoform-selectivity to avoid off-target effects. Related inhibitors of TNKSs include flavones,[15] 2-arylquinazolin-4-ones such as **2**,[16,17] isoquinolin-1-ones[18] and aryltetrahydronaphthyridinones, which maintain a classical binding mode in the nicotinamide-binding site.[19] Compound **3** (IWR-1)[20] (Fig. 1) is an inhibitor of the Wnt signaling cascade through inhibiting TNKSs, binding only to the adenosine-binding site.[20] The norbornane of **3** forces a conformational change of Tyr^{1050} (TNKS2 numbering), allowing the quinoline of **3** to π-stack with His^{1048} within this site.[21] Our previous reports of novel inhibitors include 2-aryl-8-methylquinazolin-4-ones with 4'-large or electron-withdrawing substituents (*e.g.* **2**) to provide inhibition of TNKSs (IC_{50} in the low nM range) and of Wnt / β-catenin signaling.[16,17] Some known inhibitors bind in both the nicotinamide-binding site and the adenosine-binding domain,[22,23] although the increases in potency *vs.* **1** were modest.

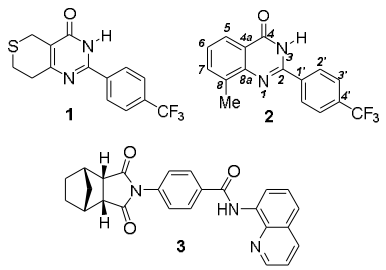

Figure 1. Examples of previously studied inhibitors of TNKSs **1**, **2** (nicotinamide-site binders) and **3** (adenosine-site binder). Inhibitor **2** is shown with locant numbers.

Here, we report the rational design and evaluation of advanced inhibitors (**13**, **14**) which maintain the 8-methylquinazolin-4-

one core and carry extensions at the 2-position to induce conformational change and binding to the adenosine-binding site, leading to a step-change in potency and isoform-selectivity. These highly potent and isoform-selective inhibitors have potential as excellent molecular probes applicable to research on diabetes and cancer.

RESULTS AND DISCUSSION

Modeling. Structural alignment of the co-crystal structures of **2** (PDB 4UFU) and **3** (PDB 3UA9) with TNKS2[17,21] provided initial insights towards the design of **13** and **14**. The quinazolinone of **2** binds in the nicotinamide-binding site, making the expected H-bonds with Ser[1068] and Gly[1032] and π-stack with Tyr[1071] (TNKS2 numbering). The quinoline of **3** is located in the adenosine-binding site, making a π-stack with His[1048] (TNKS2 numbering). Features binding at each site were linked to create chimeric compounds **13** and **14**, which combine important H-bonds and stacking interactions at both binding sites. Modeling of **13** and **14** into the active site of TNKS1 (PDB 4I9I)[23] predicted that the designed compounds could bind to the pockets in the intended way and that the length and nature of the linker were appropriate (Fig. 2). The quinazolin-4-one core could bind in the nicotinamide-binding site to make the classical H-bond and π-stacking interactions. Compounds **1** and **2** contain a 2-aryl group, which is shown to occupy a hydrophobic cavity. Modeling of **13** into TNKS1 suggests that the chosen linker could allow Tyr[1203] to move towards the nicotinamide-binding site and decrease the volume of the hydrophobic cavity. However, this shrinkage of the pocket could still allow the propanamide linker to thread through. The modeling study reveals that the linker could interact further with the protein, in that the C=O of the propanamide linker is appositely located to H-bond with the backbone NH of Tyr[1213]. Moreover, the central benzene ring and the quinoline of **13** are predicted to cause movement of His[1201] of the adenosine-binding site to place its imidazole appropriately for π-stacking with the quinoline. We have previously reported that an 8-Me group enhances inhibitory activity in the simple 2-arylquinazolinones[16,17] and related 3-arylisoquinolinones,[18] we also incorporated the 8-Me in **14**, to test if it would still make a contribution in these advanced dual-site-binding compounds (Fig. 2).

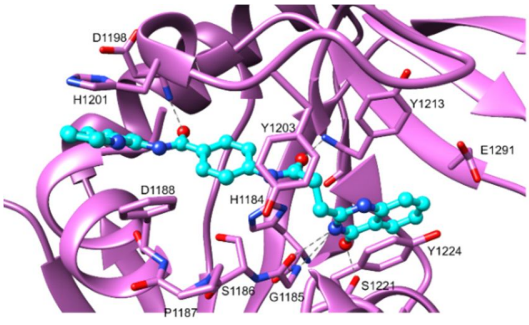

Figure 2. Model of **13** docked into the structure of TNKS1 (PDB code 4I9I).[23] The protein is shown in pink and **13** in cyan. Key H-bonds shown as grey dashed lines.

Chemical Synthesis. The synthesis of target compounds (Sch. 1) began by acylation of 8-aminoquinoline **4** with 4-nitrobenzoyl chloride to give **5**, followed by transfer hydrogenation to provide amine **6**. Anthranilamides **7** and **8**[24] were acylated with ethyl 4-chloro-4-oxobutanoate to provide **9** and **10**. One-pot cyclisation and hydrolysis in aqueous base led to the quinazolinonepropanoic acids **11** and **12**. Careful optimization of the coupling conditions was required to join **11** / **12** with **6**; simultaneous addition of the activating agent (CDI) and quinazolinones **11** / **12** to **6** was essential to provide the candidate dual-site-binding inhibitors **13** and **14** in modest yields.

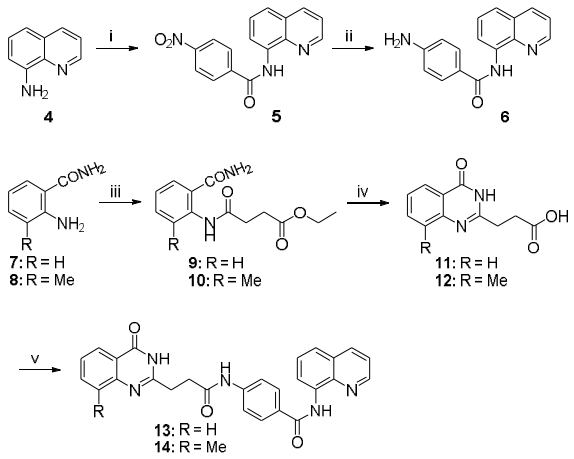

Scheme 1. Synthesis of **13** and **14**. *Reagents and conditions*: i) nitrobenzoyl chloride, pyridine, THF, 16 h, Ar; ii) $^{+}NH_4$ HCO_2^{-}, 10% Pd/C, DMF/MeOH (2:1), 2 h, Ar; iii) $EtO_2CCH_2CH_2COCl$, pyridine, THF, 16 h; iv) aq. NaOH (0.5 M), 60°C; v) 6, DMF, Pr^{i}_2NEt, carbonyldiimidazole, 72 h, Ar.

Biochemical evaluation. The target compounds **13** and **14** were evaluated *in vitro* for inhibition of TNKS1 and TNKS2 and counterscreened against eleven PARP isoforms, including the major isoform PARP1 (Table 1). Known inhibitors **1** and **3** were also examined as standards against PARP1, PARP2, TNKS1 and TNKS2. The nicotinamide-site binder **1** showed IC_{50} values in the low nanomolar range for inhibition of TNKS1 and TNKS2, which were similar to those reported by Huang *et al.*[5] However, although **1** showed reasonable selectivity for TNKS2 *vs.* PARP1 (131-fold), other comparisons called into question the use of this agent as a selective inhibitor (TNKS1 *vs.* PARP1 25-fold; TNKS1 *vs.* PARP2 4.1-fold). Compound **3**, which binds in the adenosine-binding site, had moderate activity against TNKS1 and TNKS2 (IC_{50} = 343 nM and 31 nM, respectively) and did not inhibit PARP1 or PARP2 up to 10 μM. These data are again consistent with earlier evaluations of the selectivity of this agent. Huang *et al.*[5] reported IC_{50} (TNKS2) = 56 nM and selectivity *vs.* PARP1 and PARP2 > 300-fold, while Narwal *et al.* confirmed the selectivity of **3** with IC_{50} = *ca.* 100 μM (PARP1) and IC_{50} = *ca.* 35 μM (PARP2).[21] Thus binding at the adenosine site has potential for greater selectivity for TNKSs *vs.* other PARPs, although this may not give high potency as the sole binding site.

Intermediate **6**, containing the putative adenosine-site-binding benzamidoquinoline, was evaluated for ability to bind in the absence of the anchoring quinazolin-4-one but it failed to inhibit any of the isoforms. This shows that the norbornane of **3** is essential, interacting with Tyr[1203] to modify the geometry of the adenosine-binding site to accept the benzamidoquinoline.

The candidate dual-site inhibitors **13** and **14** were shown to be extremely potent and isoform-selective inhibitors of TNKSs, inhibiting TNKS2 in the pM range and thus they are both

Table 1. IC_{50} (pIC_{50} ± standard error) values for inhibition of TNKS1, TNKS2 and PARP isoforms in biochemical assays and for inhibition of Wnt signaling in a cellular assay.

Compound	1	3	6	11	12	13	14
PARP1	854 nM (6.07 ± 0.13)	>100000 nM [a]	>100000 nM [a]	6700 nM (5.18 ± 0.17)	1000 nM (5.18 ± 0.17)	8230 nM (5.08 ± 0.12)	6500 nM (5.19 ± 0.06)
PARP2	141 nM (6.85 ± 0.08)	>100000 nM [a]	[b]	125 nM (6.90 ± 0.04)	145 nM (6.84 ± 0.12)	6900 nM (5.16 ± 0.12)	11600 nM (4.94 ± 0.05)
PARP3						40000 nM (4.40 ± 0.14)	45000 nM (4.34 ± 0.10)
PARP4						69000 nM (4.16 ± 0.10)	65000 nM (4.19 ± 0.07)
TNKS1	34 nM (7.47 ± 0.23)	343 nM (6.46 ± 0.09)	>100000 nM [a]	>100000 nM [a]	>100000 nM [a]	9.1 nM (8.04 ± 0.05)	5.1 nM (8.29 ± 0.27)
TNKS2	6.5 nM (8.19 ± 0.09)	31 nM (7.51 ± 0.10)	>100000 nM [a]	>100000 nM [a]	>100000 nM [a]	0.20 nM (9.69 ± 0.17)	0.10 nM (10.0 ± 0.05)
PARP10						>100000 nM [a]	>100000 nM [a]
PARP12						>100000 nM [a]	>100000 nM [a]
PARP14						>100000 nM [a]	>100000 nM [a]
PARP15						>100000 nM [a]	>100000 nM [a]
PARP16						>100000 nM [a]	>100000 nM [a]
Wnt	220nM (6.66 ± 0.10)	136 nM[c]				29 nM (7.54 ± 0.05)	37 nM (7.43 ± 0.06)

[a] Limited by solubility. [b] Empty cells indicate not determined. [c] Determined previously.[23]

considerably more potent than the "standard" inhibitor **1** and the adenosine-site-binder **3**. This increase in potency of inhibition of the TNKSs for **13** and **14** was not accompanied by an increase in activity against other members of the PARP family (Table 1). In particular, **13** and **14** showed very weak activity against PARP1 and PARP2 (IC_{50} >> 6 μM), leading to exquisite isoform-selectivity. Inhibitor **13** is 4.1×10^4-fold selective for TNKS2 *vs.* PARP1 and 3.5×10^4-fold selective for TNKS2 *vs.* PARP2. Similarly, **14** is 6.5×10^4-fold selective for TNKS2 *vs.* PARP1 and 11.6×10^4-fold selective for TNKS2 *vs.* PARP2. The somewhat weaker potency of these agents against TNKS1 corresponds to selectivities for TNKS1 *vs.* PARP1 and PARP2 in the range 1-2.3×10^3-fold. Thus exploiting dual-site binding with an appropriate linker makes a step-change in potency and provides isoform-selectivity with this potency. Compound **14** is approximately twice as potent as **13** against both isoforms, confirming the moderate advantage of the 8-Me on the quinazolinone core.[16,18,17] Intermediates **11** and **12**, carrying only a propanoic acid at the quinazolinone 2-position, were evaluated to explore the contribution of the quinazolinone-CH_2CH_2CO unit towards potency and selectivity; both showed no inhibition of TNKSs. We have previously shown that a 2-aryl group is required for potent inhibition of TNKSs; this requirement is thereby reinforced for inhibitors that bind only as mimics of nicotinamide.[16-19] However, **11** and **12** do inhibit PARP1 and PARP2. Previously, we showed that polar groups at the 4'-position of 2-arylquinazolin-4-ones decreased selectivity for TNKSs, in that inhibition of PARP1 was enhanced;[16-18] therefore, the 2-propanoic acid of **11** and **12** is well suited to interact with the corresponding region of protein of PARP1 that contains hydrophilic residues. Furthermore, **11** and **12** displayed moderately potent and selective inhibition of PARP2 (54- and 6.9-fold, respectively, *vs.* PARP1), results which place **11** amongst the most PARP2-selective agents known.[25] Therefore, **11** and **12** provide a new scaffold towards the development of novel PARP2-selective inhibitors.

X-ray crystallography. To rationalize the potency and isoform-selectivity of **13** and **14**, crystal structures of the compounds in complex with TNKS2 catalytic domain were solved (Supplementary information). The quinazolinone binds to the nicotinamide pocket as designed and forms interactions with the protein similar to those of **2** (PDB code 4UFU).[17] The stacking interaction with Tyr^{1071} and the H-bonds with Gly^{1032} and Ser^{1068} are preserved (Fig. 3). Binding of **3** causes opening of the active-site loop and moves His^{1048} away from the binding pocket.[21] Similar changes are observed in the crystal structures of the complexes of **13** and **14** and the quinoline binds to form an induced adenosine-binding pocket. Importantly, the H-bonds to Tyr^{1060} and to Asp^{1045}, observed in adenosine-site inhibitors,[26] are both present in the TNKS2 structures containing **13** and **14**. The central phenyl ring adopts slightly different conformations in the experimental crystal structures of **13** and **14**, indicating flexibility in the hydrophobic surface at this site. A recent dual-site binding inhibitor binds to the catalytic domain in a very similar manner (IC_{50} = 2 nM *vs.* TNKS2)[23] but does not create as efficient π-stacking interaction with His^{1201} as does the electron-poor bicycle of **13** and **14**. This may explain why compounds **13** and **14** exhibit such high inhibitory activity towards TNKSs. Unlike PARP1 and PARP2, TNKSs do not contain an α-helical regulatory domain. This domain packs against the NAD^+-binding groove and the interactions at the adenosine site contribute to the potent selectivity of the adenosine-site binders. The extreme isoform-selectivity of **13** and **14** can be rationalized, similarly to **3**, to be mainly due to the quinoline in the adenosine-binding pocket and unfavorable interactions with the charged residues present in PARP-1 and PARP-2.[17,21]

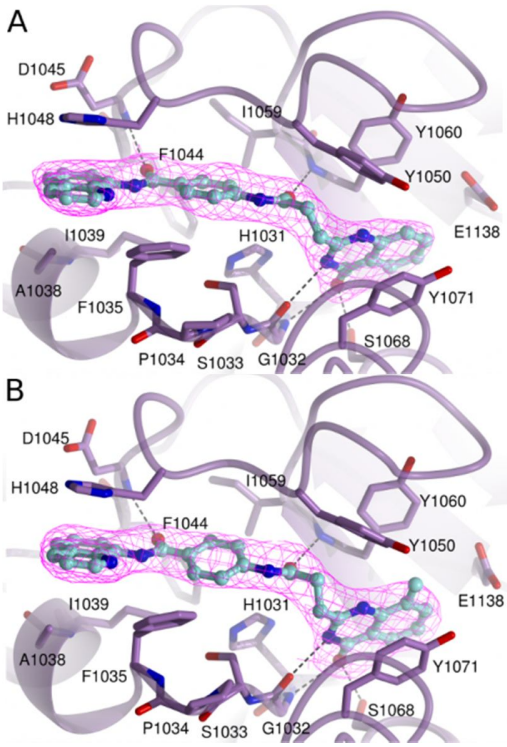

Figure 3. Crystal structure of A) TNKS2-**13** (PDB code 5FPF) and B) TNKS2-**14** (PDB code 5FPG). Hydrogen bonds are shown in dashed lines and the electron density (2mFo-DFc) is contoured at 1 Å around the ligand.

Inhibition of Wnt signaling in TCF/LEF reporter-HEK293 cells. The intracellular activity and potency of **13** and **14** was evaluated in a functional assay using a TCF/LEF Reporter-HEK293 cell line (BPS Bioscience, catalog #60501).[27] Upon extracellular Wnt signals, β-catenin is stabilized and associates with TCF/LEF transcription factors, activating transcription.[5,27] TNKSs control the stability of the β-catenin destruction complex and inhibition is expected to stabilize the destruction complex and thus lower the levels of β-catenin.[5] The TCF/LEF Reporter-HEK293 cell line is used to measure this interference with this pathway. Both **13** (IC_{50} = 29 nM) and **14** (IC_{50} = 37 nM) were shown to be extremely effective and potent cellular inhibitors of Wnt / β-catenin signaling, confirming their uptake into cells and their activity therein (Table 1). Thus **13** and **14** are *ca*. 10× more potent in cells than the standard inhibitor **1**, reflecting the greater potency of the dual-site inhibitors *in vitro*. Cell viability was monitored with a light microscope; **13** and **14** were not cytotoxic in this assay.

Anti-proliferative activity towards DLD-1 human colon carcinoma cells. Aberrant Wnt signaling is found in > 90% of colorectal cancers, owing to mutation in the APC protein which is a component of the β-catenin destruction complex.[6] Compound **1** has been reported to have anti-proliferative activity against DLD-1 human colon cancer cells but only under serum-deprived conditions.[5,28] Using a colony-forming assay, **13** and **14** were shown to inhibit formation of colonies of DLD-1 cells even under normal-serum conditions (Fig. 4) at 100 nM and 1.0 μM, conditions under which **1** was inactive. This observation again reflects the greater potency of **13** and **14** *in vitro* and in cells.

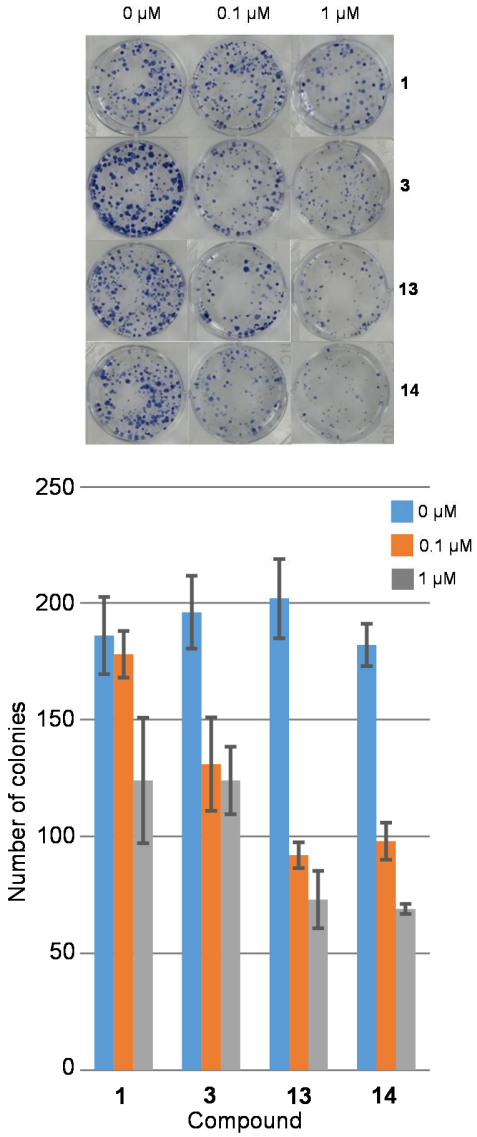

Figure 4. Upper: Exemplary image of DLD-1 colony forming assay (1000 cells/well) with **1**, **3**, **13** and **14** (0 μM (control with 1% DMSO v/v only), 1.0 μM and 100 nM). **Lower**: Histogram of data from assay. **1**, **3**, **13** and **14** (n = 3).

Insulin-stimulated glucose uptake. The axin-TNKS-KIF3A complex is stabilized through inhibition of TNKS.[12] Ablation of expression of TNKSs has been reported to upregulate GLUT4 at the post-transcriptional level, potentially increasing uptake of glucose into adipocytes.[14] To address this pharmacologically, **13** and **14** were examined for their ability to enhance insulin-stimulated uptake of glucose. 3T3-L1 Adipocytes were treated with **13** and **14** in the presence of insulin (100 nM).[29] Compound **1** was used for comparison as the current "standard" TNKS inhibitor. The insulin-stimulated uptake of radiolabeled 2-deoxy-D-glucose into the cells was measured. The weaker TNKS inhibitor **1** had no effect on insulin-stimulated glucose uptake in comparison to the insulin-only control. The slight decrease in non-stimulated glucose uptake in presence of **1** (1.0 μM) was not significantly different from control. Non-stimulated glucose uptake in presence of **13** and **14** (1.0 μM) was not significantly different from control. In comparison to insulin only and with

1, both **13** and **14** significantly further increased insulin-stimulated glucose uptake. Glucose uptake increased by *ca*. 40% and 20% using 100 nM and 1.0 μM of **13**, respectively. Insulin-stimulated uptake of glucose increased by *ca*. 20% by **14** at 100 nM and 1.0 μM in comparison to insulin treatment only (Fig. 5). This confirms potent intracellular activity of **13** and **14**.

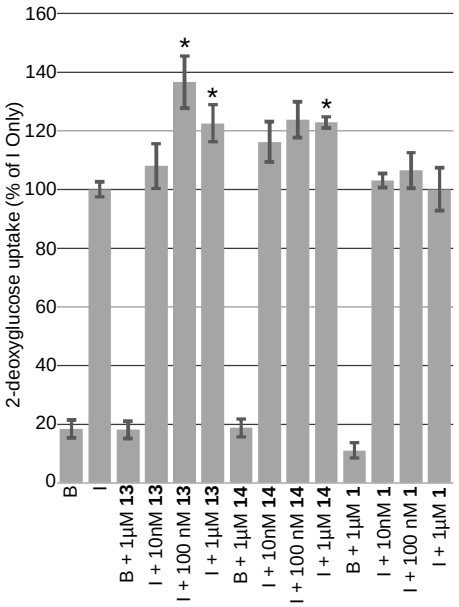

Figure 5. Effect of **1**, **13** and **14** on % insulin-stimulated glucose uptake in 3T3-L1 adipocytes. Basal levels (B) with or without compound contain no insulin (I). I (with and without compound) administered at final concentration 100 nM. Results are mean and SEM relative to I only (n = 3 for **1** and n = 5 for **13** and **14**). I + 100 nM 13 vs. I p = 0.02; I + 1.0 μM **13** vs. I p = 0.02; I + 100 nM **14** vs. I p = 0.07; I + 1.0 μM **14** vs. I p = 0.01; B vs. B + **13** p = 0.98; B vs. B + **14** p = 0.94; B vs. B + **1** p = 0.21.

CONCLUSION

In this paper, we disclose the design, synthesis and evaluation of two new highly potent and isoform-selective TNKS inhibitors, **13** and **14**. Crystal structures of these compounds bound into the catalytic domain of TNKS2 confirmed that, as designed, the quinazolin-4-one moiety occupied the nicotinamide-binding site, setting up the linker so that the quinoline moiety interacts with the adenosine-binding region. This dual-site design has led to the most potent and isoform-selective inhibitors reported to date, with IC_{50} = 100 pM for inhibition of TNKS2 by **14** and 1.2×10^5-fold selectivity for inhibition of TNKS2 *vs*. the major PARP isoform, PARP1. Cellular uptake of these agents was demonstrated by their potent inhibition of Wnt / β-catenin signaling in the low nM range. Significant anti-proliferative activity was demonstrated in DLD-1 human colon carcinoma cells at 100 nM under normal serum conditions. For the first time, truly potent and selective TNKS inhibitors are shown to increase insulin-stimulated glucose uptake, whereas previous studies have used non-selective pan-PARP inhibitors;[13] this provides further evidence of a role of TNKSs in insulin-stimulated glucose transport and further studies will elucidate the mechanisms of this activation, presumably through the axin-TNKS-KIF3A complex.[12] In comparative studies *in vitro*, the widely-used TNKS inhibitor **1** has been shown to be markedly less potent than **13** and **14** and to lack the exquisite isoform-selectivity of these new agents. The improved potency and isoform-selectivity of **13** and **14** is manifest in three comparative cellular functional assays, where they show useful activity in situations where **1** lacks potency or activity.

Compounds **13** and **14** are now available as potent and isoform-selective TNKS inhibitors which inhibit the Wnt response pharmacologically in cells. They will have applications as molecular tools in studies on Wnt and related systems. These results also indicate that inhibition of TNKSs can increase sensitivity of cells to insulin, with potential application in Type-2 diabetes, as high doses of insulin can cause dysregulation of various signaling cascades (PI3K / Akt / mTOR).[30] Antiproliferative activity has also been demonstrated in human colon cancer cells under normal serum conditions, supporting TNKS as a therapeutic target in the many cancers with aberrant Wnt signaling. A new structural scaffold (**11**, **12**) for selective inhibitors of PARP2 has also been identified.

EXPERIMENTAL SECTION

Chemistry

The purity of target compounds were >95% as determined by ^{1}H and ^{13}C NMR, high resolution mass spectrometry using electrospray ionization and HPLC analysis at two different wavelengths (see supplementary information for general experimental, spectra of all compounds and synthetic procedures of intermediate compounds).

Synthesis of target compounds 13 and 14.

2-(3-Oxo-3-(4-((quinolin-8-yl)aminocarbonyl)phenylamino)propyl)quinazolin-4-one (13). Compound **6** (548 mg, 2.08 mmol) in dry DMF (50 mL) was treated with Pr^i_2NEt (2.96 g, 22.9 mmol), then carbonyldiimidazole (371 mg, 2.29 mmol), followed by addition of **11** (500 mg, 2.29 mmol). The mixture was stirred for 72 h under Ar. The solvent was evaporated and the residue was dissolved in EtOAc/MeOH (1:2, 70 mL). The organic solution was washed with water (3 × 30 mL) and brine (3 × 30 mL), then dried. Evaporation and chromatography (1:9 EtOAc / CH_2Cl_2 → 1:9 MeOH / EtOAc) gave a mixture containing **13**. Further chromatography (EtOAc) gave **13** (74 mg, 8%) as a pale purple solid: mp 265-268°C ^{1}H NMR ($(CD_3)_2SO$) δ 2.95-2.98 (4 H, m), 7.47 (1 H, t, *J* = 7.0 Hz), 7.63 (1 H, d, *J* = 8.0 Hz), 7.64-7.69 (2 H, m), 7.72-7.83 (2 H, m), 7.82 (2 H, d, *J* = 8.5 Hz), 8.00 (2 H, d, *J* = 8.5 Hz), 8.08 (1 H, d, *J* = 8.0 Hz), 8.46 (1 H, dd, *J* = 8.0, 1.5 Hz), 8.72 (1 H, d, *J* = 7.5 Hz), 8.97 (1 H, dd, *J* = 4.0, 1.5 Hz), 10.45 (1 H, s), 10.59 (1 H, s), 12.27 (1 H, s); ^{13}C NMR ($(CD_3)_2SO$) δ 29.09, 32.34, 116.44, 118.70, 120.93, 122.13, 122.38, 125.77, 126.04, 126.76, 127.11, 127.86, 128.12, 128.44, 134.16, 134.35, 136.81, 138.26, 142.76, 148.74, 149.18, 156.52, 161.64, 163.96, 170.73; MS *m/z* 464.1722 $[M + H]^+$ ($C_{27}H_{22}N_5O_3$ requires 464.1723).

8-Methyl-2-(3-oxo-3-(4-((quinolin-8-yl)aminocarbonyl)phenylamino)propyl)quinazolin-4-one (14). Compound **6** (514 mg, 1.95 mmol) in dry DMF (50 mL) was treated with Pr^i_2NEt (2.78 g, 21.5 mmol), then carbonyldiimidazole (348 mg, 2.15 mmol), followed by addition of **12** (500 mg, 2.15 mmol). The mixture was stirred for 72 h under Ar. The solvent was evaporated and the residue was dissolved in EtOAc/MeOH (1:2, 70 mL). The solution was washed with water (3 × 30 mL) and brine (3 × 30 mL), then dried. Evaporation and chromatography (1:9 EtOAc / CH_2Cl_2 → EtOAc) gave **14** (119 mg, 21%) as a beige solid: mp 280-282°C; ^{1}H NMR ($(CD_3)_2SO$) δ 2.44 (3H, s), 2.93

(2 H, t, *J* = 6.0 Hz), 3.01 (2 H, t, *J* = 7.0 Hz), 7.31 (1 H, t, *J* = 7.5 Hz), 7.58 (1 H, m), 7.63-7.69 (2 H, m), 7.70 (1 H, dd, *J* = 8.5, 1.0 Hz), 7.83 (2 H, d, *J* = 8.5 Hz), 7.91 (1 H, dd, *J* = 8.0, 1.0 Hz), 8.00 (2 H, d, *J* = 8.5 Hz), 8.46 (1 H, dd, *J* = 8.5, 2.0 Hz), 8.72 (1 H, dd, *J* = 7.5, 1.5 Hz), 8.97 (1 H, dd, *J* = 4.5, 2.0 Hz), 10.76 (1 H, s), 10.59 (1 H, s), 12.25 (1 H, s); ^{13}C NMR ($(CD_3)_2SO$) δ17.06, 28.99, 32.08, 116.45, 118.67, 120.76, 122.11, 122.38, 123.36, 125.44, 127.11, 127.86, 128.09, 128.34, 134.17, 134.59, 134.84, 136.81, 138.26, 142.91, 147.07, 149.17, 155.12, 161.94, 163.98, 170.98; MS *m/z* 478.1876 $[M + H]^+$ ($C_{28}H_{24}N_5O_3$ requires 478.1879).

Counter-screening against PARP3, PARP4, PARP10, PARP12, PARP14, PARP15 and PARP16. Compounds **13** and **14** were counter-screened for inhibition of these isoforms using methods described previously.[31, 32] The new inhibitors show no structural alerts for PAINS and are colorless and non-fluorescent.

Insulin-stimulated glucose uptake. 3T3-L1 fibroblasts (from the American Type Culture Collection), were cultured in DMEM and differentiated to adipocytes by treatment with insulin, dexamethasone and isobutylmethylxanthine, as described previously.[29] On the day of the experiment, 10-12 d post-differentiation, the cells were incubated with serum-free DMEM for 2 h at 37°C. Cells in the treatment group were treated with increasing concentrations of **13** or **14** for 1 h. At the end of the incubation period, the cells were washed thrice with Krebs-Ringer-HEPES (KRH) buffer (140 mM NaCl, 4.7 mM KCl, 2.5 mM $CaCl_2$, 1.25 mM $MgSO_4$, 2.5 mM NaH_2PO_4, 10 mM HEPES, (pH 7.4)) and incubated for 30 min with **13** or **14** and in either the absence or presence of insulin (100 nM) at 37°C. After the 30 min incubation period, 2-deoxy-D-[2,6-^{3}H]glucose (final concentration 50 μM, 0.1 μCi well^{-1}) was added for 5 min and the cells were washed four times with ice-cold KRH buffer. Nonspecific uptake of 2-deoxy-D-glucose was measured in the presence of 10 μM cytochalasin B. The cells were lysed in aq. NaOH (0.1 M) and radioactivity was counted in a TriCarb Packard scintillation counter (Perkin-Elmer). The concentrations of proteins were measured using BCA protein assay kit (Thermo Fisher Scientific). Results were calculated as nmol of 2-deoxy-D-glucose min^{-1} (mg protein)$^{-1}$ and are expressed as % of insulin-only control. Statistical analysis; results were analyzed using two-tailed paired t tests.

AUTHOR INFORMATION

Corresponding Author

* Phone +44 (0)1225 383379. E-mail: A.Nathubhai@bath.ac.uk.

Author Contributions

The manuscript was written through contributions of all authors. The authors declare no competing financial interest.

Accession codes

Coordinates and structure factors are deposited at the Protein Data Bank with codes 5FPF and 5FPG. Authors will release the atomic coordinates and experimental data upon article publication.

ACKNOWLEDGMENT

We acknowledge the support from the European Synchrotron Radiation Facility (ESRF, Grenoble, France). We are grateful to Local Contracts at ESRF for providing assistance in using beamlines ID23-1 and ID29. We thank Dr. Silvia Muñoz-Descalzo (University of Bath) and Dr. Penelope C. Hayward (University of Cambridge) for helpful discussions.

Funding Sources

The research was funded by Worldwide Cancer Research (Grant No. 13-1021 to AN, MDL, DT and MDT), MRC UK (Grant No. MR/J003417/1) to FK and GDH), Biocenter Oulu, Academy of Finland (287063 and 294085 to LL and TH) and the Center of Excellence Grant 2012-2017 of the Academy of Finland (284605 to TP).

ABBREVIATIONS

NAD^+, Nicotinamide Adenosine Dinucleotide; ADP, Adenosine diphosphate; GLUT4, Glucose Transporter Type-4; CDI, N,N'-Carbonyldiimidazole; IC_{50}, half-maximal inhibitory concentration; PDB, Protein Data Bank; TCF, T-cell factor; LEF, Lymphoid Enhancer-binding Factor; DMEM, Dulbecco's Modified Eagle Medium; BCA, Bicinchoninic acid.

ASSOCIATED CONTENT

Supporting Information. Synthetic details, ^{1}H NMR, ^{13}C NMR, HRMS, HPLC, TNKS1 enzyme assay method, TNKS1 IC_{50} graphs, TNKS2 enzyme assay method, TNKS2 IC_{50} graphs, PARP1 enzyme assay method, PARP1 IC_{50} graphs, PARP2 enzyme assay method, PARP2 IC_{50} graphs, Wnt signaling inhibition cellular assay method, Wnt signaling inhibition IC_{50} graphs, X-ray crystallography refinement data, colony-forming cellular assays experimental and Molecular Formula Strings. This material is available free of charge via the Internet at http://pubs.acs.org.

REFERENCES

1) Ferris, D. V. Evolution of poly(ADP-ribose) polymerase-1 (PARP-1) inhibitors. *J. Med. Chem*. **2010**, *53*, 4561-4584.
2) Mi Kyung, K.; Smith, S. Persistent telomere cohesion triggers a prolonged anaphase. *Mol. Biol. Cell* **2014**. *25*, 30-40.
3) Smith, S.; Giriat, I.; Schmitt, A.; de Lange, T. Tankyrase, a poly(ADP-ribose) polymerase at the human telomeres. *Science*, **1998**, *282*, 1484-1487.
4) Chang, W.; Dynek, J. N.; Smith, S. NuMA is a major acceptor of poly(ADP-ribosyl)ation by tankyrase 1 in mitosis. *Biochem. J.* **2005**, *391*, 177-184.
5) Huang, S.-M. A.; Mishina, Y. M.; Liu, S.; Cheung, A.; Stegmeier, F.; Michaud, G. A.; Charlat, O.; Wiellette, E.; Zhang, Y.; Wiessner, S.; Hild, M.; Shi, X.; Wilson, C. J.; Mickanin, C.; Myer, V.; Fazal, A.; Tomlinson, R.; Serluca, F.; Shao, W.; Cheng, H.; Shultz, M.; Rau, C.; Schirle, M.; Schlegl, J.; Ghidelli, S.; Fawell, S.; Lu, C.; Curtis, D.; Kirschner, M. W.; Lengauer, C.; Finan, P. M.; Tallarico, J. A.; Bouwmeester, T.; Porter, J. A.; Bauer, A.; Cong, F. Tankyrase inhibition stabilizes axin and antagonizes Wnt signalling. *Nature*, **2009**, *461*, 614-620.
6) White, B. D.; Chien, A. J.; Dawson, D. W. Dysregulation of Wnt/β-catenin signaling in gastrointestinal cancers. *Gastroenterology*, **2012**, *142*, 219-232.
7) Katoh, M.; Kirikoshi, H.; Terasaki, H.; Shiokawa, K. *WNT2B2* mRNA, up-regulated in primary gastric cancer, is a positive regulator of the WNT-β-catenin-TCF signaling pathway. *Biochem. Biophys. Res. Commun.* **2001**, *289*, 1093-1098.
8) Miyoshi, Y.; Iwao, K.; Nagasawa, Y.; Aihara, T.; Sasaki, Y.; Imaoka, S.; Murata, M.; Shimano, T.; Nakamura, Y. Activation of the β-catenin gene in primary hepatocellular carcinomas by somatic alterations involving exon 3. *Cancer Res.* **1998**, *58*, 2524-2527.
9) Katoh M. Expression and regulation of WNT1 in human cancer: Up-regulation of WNT1 by β-estradiol in MCF-7 cells. *Int. J. Oncol.* **2003**, *22*, 209-212.
10) McGonigle, S.; Chen, Z-H.; Wu, J-Y.; Chang, P.; Kolber-Simonds, D.; Ackermann, K.; Twine, N. C.; Shie, J. L.; Miu, J. Z. T.; Huang, K. C.; Moniz, G. A.; Nomoto, K. E7499: A dual inhibitor of

PARP1/2 and tankyrase1/2 inhibits growth of DNA repair deficient tumors and antagonizes Wnt signalling. *Oncotarget*, **2015**, *6*, 41307-41323.
11) Shikata, K.; Ninomiya, T.; Kiyohara, Y.; Diabetes mellitus and cancer risk: review of the epidemiological evidence. *Cancer Sci.* **2013**. *104*, 9-14.
12) Guo, H.-L.; Zhang, C.; Liu, Q.; Li, Q. X; Lian, G.; Wu, D.; Li, X.; Zhang, W.; Shen, Y.; Ye, Z.; Lin, S.-Y.; Lin, S.-C. The Axin/TNKS complex interacts with KIF3A and is required for insulin-stimulated GLUT4 translocation. *Cell. Res.* **2012**, *22*, 1246-1257.
13) Yeh, T-Y. J.; Sbodio, I. J.; Tsun, Z-Y.; Lou, B.; Chi, N-W. Insulin-stimulated exocytosis of GLUT4 is enhanced by IRAP and its partner tankyrase. *Biochem. J.* **2007**, *402*, 279-290.
14) Yeh, T-Y. J.; Beiswenger, K. K.; Li, P.; Bolin, K. E.; Lee, R. M.; Tsao, T-S.; Murphy, A. N.; Henever, A. L.; Chi, N-W. Hypermetabolism, hyperphagia, and reduced adiposity in tankyrase-deficient mice. *Diabetes*, **2009**, *58*, 2476-2485.
15) Narwal, M.; Haikarainen, T.; Fallarero, A.; Vuorela, P. M.; Lehtiö, L. Screening and structural analysis of flavones inhibiting tankyrases. *J. Med. Chem*. **2013**, *56*, 3507-3517.
16) Nathubhai, A.; Wood, P. J.; Lloyd, M. D.; Thompson, A. S.; Threadgill, M. D. Design and discovery of 2-arylquinazolin-4-ones as potent and selective inhibitors of tankyrases. *ACS Med. Chem. Lett.* **2013**, *4*, 1173-1177.
17) Paine, H. A.; Nathubhai, A.; Woon, E. C. Y.; Sunderland, P. T.; Wood, P. J.; Mahon, M. F.; Lloyd, M. D. Thompson, A. S.; Haikarainen, T.; Narwal, M.; Lehtiö, L.; Threadgill, M. D. Exploration of the nicotinamide-binding site of the tankyrases, identifying 3-arylisoquinolin-1-ones as potent and selective inhibitors in vitro. *Bioorg. Med. Chem*. **2015**, *23*, 5891-5908.
18) Kumpan, K.; Nathubhai, A.; Zhang C.; Wood, P. J.; Mahon, M. F.; Lloyd, M. D.; Thompson, A. S.; Haikarainen, T.; Lehtiö, L.; Threadgill, M. D. Structure-based design, synthesis and evaluation in vitro of arylnapthyridinones, arylpyridopyrimidinones and their tetrahydro derivatives as inhibitors of the tankyrases. *Bioorg. Med. Chem*. **2015**, *23*, 3013-3032.
19) Gunaydin, H.; Gu, Y.; Huang, X. Novel binding mode of a potent and selective tankyrase inhibitor. *Plos One*, **2012**, *7*, e33740.
20) Narwal, M.; Venkannagari, H.; Lehtiö, L. Structural basis of selective inhibition of human tankyrases. *J. Med. Chem*. **2012**, *55*, 1360-1367.
21) Nathubhai, A.; Wood, P. J.; Haikarainen, T.; Hayward, P. C.; Muñoz-Descalzo, S.; Thompson, A. S.; Lloyd, M. D.; Lehtiö, L.; Threadgill, M. D. Structure-Activity Relationships of 2-arylquinazolin-4-ones as highly selective and potent inhibitors of tankyrases. *Eur. J. Med. Chem.*, **2016**, *118*, 316-327.
22) Shultz, M. D.; Cheung, A. K.; Kirby, C. A.; Firestone, B.; Fan, J.; Chen, C. H.-T.; Chen, Z.; Chin, D. N.; DiPietro, L.; Fazal, A.; Feng, Y.; Fortin, P. D.; Gould, T.; Lagu, B.; Lei, H.; Lenoir, F.; Majumdar, D.; Ochala, E.; Palermo, M. G.; Pham, L.; Pu, M.; Smith, T.; Stams, T.; Tomlinson, R. C.; Touré, B. B.; Visser, M.; Wang, R. M.; Waters, N. J.; Shao, W. Identification of NVP-TNKS656: The use of structure–efficiency relationships to generate a highly potent, selective, and orally active tankyrase inhibitor. *J. Med. Chem*. **2013**, *56*, 6495-6511.
23) Bregman. H.; Gunyadin. H.; Gu. Y.; Schneider. S.; Wilson. C.; DiMauro. E. F.; Huang. X. Discovery of a class of novel tankyrase inhibitors that bind to both the nicotinamide pocket and the induced pocket. *J. Med. Chem*. **2013**, *56*, 1341-1345.
24) Nathubhai, A.; Patterson, R.; Woodman, T. J.; Sharp, H. E. C.; Chui, M. T. Y.; Chung, H. H. K.; Lau, S. W. S.; Zheng, J.; Lloyd, M. D.; Thompson, A. S.; Threadgill, M. D. N^3-Alkylation during formation of quinazolin-4-ones from condensation of anthranilamides and orthoamides. *Org. Biomol. Chem*. **2011**, *9*, 6089-6099.
25) Sunderland, P. T.; Woon, E. C. Y.; Dhami, A.; Bergin, A. B.; Mahon, M. F.; Wood, P. J.; Jones, L. A.; Tully, S. R.; Lloyd, M. D.; Thompson, A. S.; Javaid, H.; Martin, N. M. B.; Threadgill, M. D. 5-Benzamidoisoquinolin-1-ones and 5-(ω-carboxyalkyl)isoquinolin-1-ones as isoform-selective inhibitors of poly(ADP-ribose)polymerase-2 (PARP-2). *J. Med. Chem*. **2011**, *54*, 2049-2059.
26) Haikarainen, T.; Waaler, J.; Ignatev, A.; Nkizinkiko, Y.; Venkannagari, H.; Obaji, E.; Krauss, S.; Lehtiö, L. Development and structural analysis of adenosine site binding tankyrase inhbitors. *Bioorg. Med. Chem. Lett.* **2016**, *26*, 328-333.
27) Haikarainen, T.; Koivunen, J.; Narwal. M.; Venkannagari, H.; Obaji, E.; Joensuu, P.; Pihlajaniemi, T.; Lehtiö, L. *Para*-substituted 2-phenyl-3,4-dihydroquinazolin-4-ones as potent and selective tankyrase inhibitors. *ChemMedChem*, **2013**, *8*, 1978-1985.
28) Bao, R; Christova, T.; Song, S.; Angers, S.; Yan, X.; Attisano, L. Inhibition of tankyrases induces axin stabilization and block Wnt signalling in breast cancer cells. *PloS One*, **2012**, *7*, e48670.
29) Frost, S. C.; Lane, M. D. Evidence for the involvement of vicinal sulfhydryl-groups in insulin-activated hexose-transport by 3T3-L1 adipocytes. *J. Biol. Chem*. **1985**, *260*, 2646-2652.
30) Othman, E. M.; Hintzsche, H.; Stopper, H. Signalling steps in the induction of genomic damage by insulin in colon and kidney cells. *Free. Rad. Biol. Med.* **2014**, *68*, 247-257.
31) Venkannagari, H.; Verheugd, P.; Koivunen, J.; Pihlajaniemi, T.; Lüscher, B.; Lehtiö, L. Small-molecule chemical probe rescues cells from mono-ADP-ribosyltransferase ARTD10/PARP10-induced apoptosis and sensitizes cancer cells to DNA damage. *Cell Chem. Biol.* **2016**, *23*, 1251-1260.
32) Venkannagari, H.; Fallarero, A.; Feijs, K. L. H.; Lüscher, B.; Lehtiö, L. Activity-based assay for human mono-ADP-ribosyltransferase ARTD7/PARP15 and ARTD10/PARP10 aimed at screening and profiling inhibitors. *Eur. J. Pharm. Sci.* **2013**, *49*, 148-156.

Table of Contents graphic

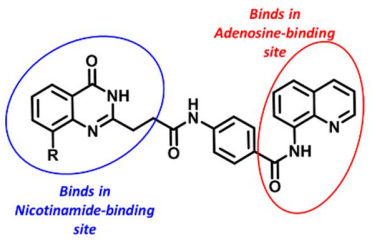

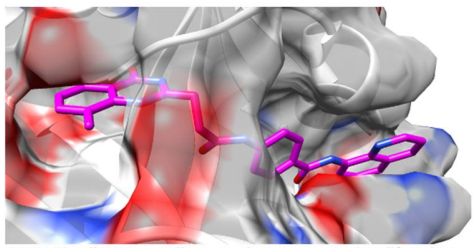

R	TNKS1 IC_{50}	TNKS2 IC_{50}	PARP1 IC_{50}	PARP2 IC_{50}	HEK293 cell Wnt IC_{50}	Adipocyte glucose uptake (@100nM)	Antiproliferative DLD-1 (@ 100nM)
H	9.1nM	0.20nM	8.2μM	6.9μM	29nM	↑ 20-40%	✓
CH_3	5.1nM	0.10nM	6.5μM	11.6μM	37nM	↑ 20%	✓